Characterization of Metal-Oxide Catalysts in Operando *Conditions by Combining X-ray Absorption and Raman Spectroscopies in the Same Experiment*

A. Patlolla, P. Baumann, W. Xu, S. D. Senanayake, J. A. Rodriguez & A. I. Frenkel

Topics in Catalysis

ISSN 1022-5528

Top Catal
DOI 10.1007/s11244-013-0053-y

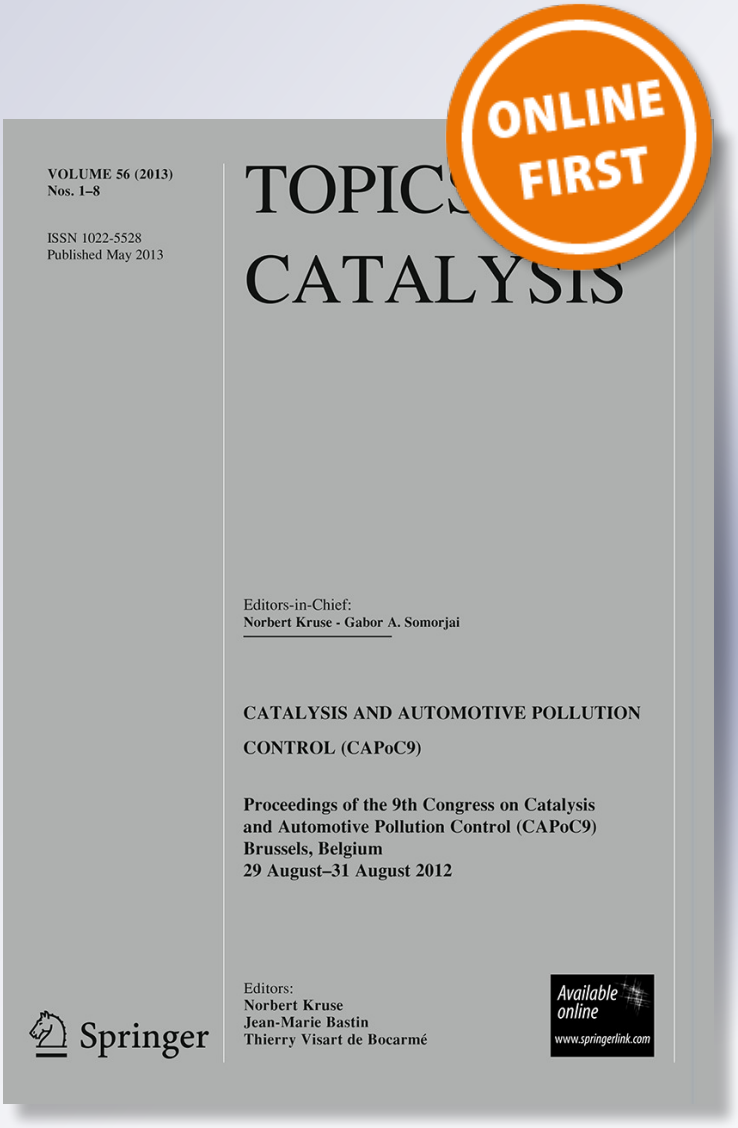

Springer

Top Catal
DOI 10.1007/s11244-013-0053-y

ORIGINAL PAPER

Characterization of Metal-Oxide Catalysts in *Operando* Conditions by Combining X-ray Absorption and Raman Spectroscopies in the Same Experiment

A. Patlolla · P. Baumann · W. Xu · S. D. Senanayake · J. A. Rodriguez · A. I. Frenkel

Abstract We have developed a new instrumental setup that combines simultaneous X-ray absorption spectroscopy, Raman spectroscopy and online mass spectrometry for *operando* studies of catalytic reactions. The importance of combining these techniques in the same experiment is demonstrated with the example of CO oxidation over nanoscale copper oxide catalysts supported on high surface area titanium oxide. X-ray absorption near edge structure (XANES) spectroscopy provides information on the charge state and local geometry of the catalytically active atoms. Extended X-ray absorption fine-structure (EXAFS) technique adds information about their local coordination environment. Raman spectroscopy adds sensitivity to crystallographic phase and long range order that both XANES and EXAFS are lacking. Together, these measurements enable simultaneous studies of the structural and electronic properties of all components present in metal-oxide catalysts. Coupled with online reactant and product analysis, this new setup allows one to elucidate the synergy between different components of a catalytic system and shed light on its catalytic activity and selectivity.

A. Patlolla · P. Baumann · A. I. Frenkel (✉)
Physics Department, Yeshiva University, 245 Lexington Avenue, New York, NY 10016, USA
e-mail: Anatoly.Frenkel@yu.edu

P. Baumann
University of Applied Sciences of Northwestern Switzerland, 4132 Muttenz, Switzerland

W. Xu · S. D. Senanayake · J. A. Rodriguez
Department of Chemistry, Brookhaven National Laboratory, Upton, NY 11973, USA

Published online: 18 May 2013

Keywords Multi-technique characterization · *Operando* studies · Metal Oxide catalysts · Oxygen reservoir

1 Introduction

Transition metal oxide-supported catalysts are among the most ubiquitous catalytic systems commonly used [1–6]. Despite significant progress made in developing catalysis theories where completely [7] or partially [8, 9] reduced oxides play a central role in the catalytic process, the role of the oxide support is relatively less understood. One of the main challenges towards a more objective investigation is the need to study all components of metal-oxide catalysts in the same conditions, which is difficult to accomplish when different techniques are used. Within the field of spectroscopy alone, a large number of techniques such as XAS [10], NMR [11], EPR [12], IR [13], Raman [14] and UV–VIS [15] have already been adapted to study metal-oxide catalysts under reaction conditions, providing complementary information about the catalytic process and structure of the catalyst. However, the challenge remains in the co-interpretation of their results since these methods are commonly applied in separate setups to the samples exposed to different experimental conditions and possessing different degrees of heterogeneity. With the development of advanced characterization techniques to monitor catalytic reactions *in operando*, new instrumentation for multi-technique characterization has been built [16–28].

In this article, we present a new experimental setup, which combines two spectroscopic techniques, XAS and Raman, coupled to a mass-spectrometer (MS) for reactant and product analysis. This instrument is available at the Synchrotron Catalysis Consortium that helps to operate

beamlines X18B, X19A and X18A at the National Synchrotron Light Source at Brookhaven National Laboratory for investigations of time-resolved and temperature-resolved catalytic reactions in fixed-bed catalytic reactors. Two modifications of XAS, namely, the X-ray absorption near edge structure (XANES) and extended X-ray absorption fine structure (EXAFS) are excellent methods to measure local electronic and atomic configuration of metal atoms in a catalyst. XANES and EXAFS experiments can be done in situ and *in operando* during the catalytic reaction. Raman spectroscopy is highly complementary to XANES and EXAFS studies, due to its sensitivity to the structure of surface oxides and the oxide support material, as well as their transformations during the reaction process. Since XAS provides short range information only, it is not sensitive to such effects that occur in the long range, i.e., tens of nanometers. Raman spectroscopy, on the other hand, is not limited to the short range order, and despite an inability to detect the metallic phase, it is an excellent tool for studies of oxides. Hence, by combining XAS and Raman to study the same catalytic process, one can elucidate changes that occur simultaneously at different length scales in the course of the reaction and arrive at a better understanding of their synergy in any catalytic mechanism than when these measurements are undertaken separately.

We report here our experimental setup and a demonstration of its capabilities by using as a case study the catalytic oxidation of CO over a 5 wt% CuO/TiO_2 catalyst. Copper oxides supported on TiO_2 are attractive heterogeneous catalysts and have been widely used in the industry for selective oxidation of *o*-xylene to phthalic anhydride [29, 30], steam reforming and methanol dehydrogenation [31, 32], CO oxidation [33, 34], NO*x* decomposition [33], and the complete mineralization of a variety of volatile organic compounds (VOCs) [35]. The nature of the active state of Cu in CO oxidation and, hence, its mechanism are far from being completely understood. Our work provides new insights into this field by illuminating a reaction pathway from several different perspectives (XANES, EXAFS, Raman and MS). We have also observed activity of this catalyst for the CO oxidation when studied under a CO/H_2O mixture, and highlighted the possible role of TiO_2 as an oxygen reservoir when the catalyst is reduced, in agreement with previous studies of support systems acting as a source of oxygen [36].

2 Experimental

2.1 Catalyst Preparation

Anatase TiO_2 was calcined to 500 °C in air flow prior to incorporating a cupric nitrate precursor ($Cu(NO_3)_2$). The 5 wt% CuO/TiO_2 catalyst was prepared by a deposition–precipitation method (DP) using Na_2CO_3 as the precipitating agent, which was added to the TiO_2 and Cu precursor in order to keep a pH neutral (=7) at 70 °C. In these conditions, the copper precipitated as $Cu(OH)_2$. The CuO/TiO_2 sample was calcined to 500 °C in air flow following the DP process. The experiments of reduction of the CuO/TiO_2 in CO and the catalytic oxidation of CO were done at temperatures (<300 °C) much lower than the one used for the calcination process (500 °C).

2.2 Catalytic Activity

Operando experiments were performed in a Clausen cell [37] which allows for the flow of reactant gases over the sample during the acquisition of XAS and Raman data (Fig. 1). The sample powder was loosely packed into a 1.0 mm O.D./0.9 mm I.D. quartz capillary. The capillary was connected to 1/16 in Swagelok style fittings with Vespel ferrules. An Omega thermocouple was inserted into the capillary and placed adjacent to, and contacting the catalyst bed. The sample was aligned so that its portion closest to the thermocouple was simultaneously in the beam path for X-ray measurements and at the focus spot from the Raman optical probe. The reagent gases were passed into the quartz tube through an inlet and the products were analyzed by using a mass spectrometer connected through an outlet. The catalyst sample was heated by using a resistive heater placed under the catalyst bed. The 5 wt% CuO/TiO_2 samples were initially treated with helium at a flow rate of 10 ml/min. Three different experiments were performed with different samples from the same batch: (1) Reduction of the supported Cu oxide under a 5 % CO/He flow during a temperature ramp between 25 and 250 °C, (2) CO oxidation reaction under a 0.5 %CO/0.25 $\%O_2$/He mixture in the same temperature regime, and (3) investigation of the catalytic activity for water–gas shift reaction. In all cases, the flow rate of the gas feed was 10 ml/min. Each experiment took a few hours, and during the entire process the reaction products were monitored with a mass spectrometer.

The mass spectrometer used to monitor the composition of the reacting gases at the outlet of the reactor covered the 0–100 amu range (QMS, Stanford Research Systems). A portion of the exit gas flow passed through a leak valve and into the QMS vacuum chamber. QMS signals at mass-to-charge (m/z) ratios of 2(H_2), 4 (He), 18 (H_2O), 28 (CO), and 44 (CO_2) were monitored during the experiments, and these were recorded at the same time by a computer.

2.3 X-ray Absorption Spectroscopy

Cu K-edge XAS data were collected in transmission mode at the beamline X19A using ionization chamber detectors

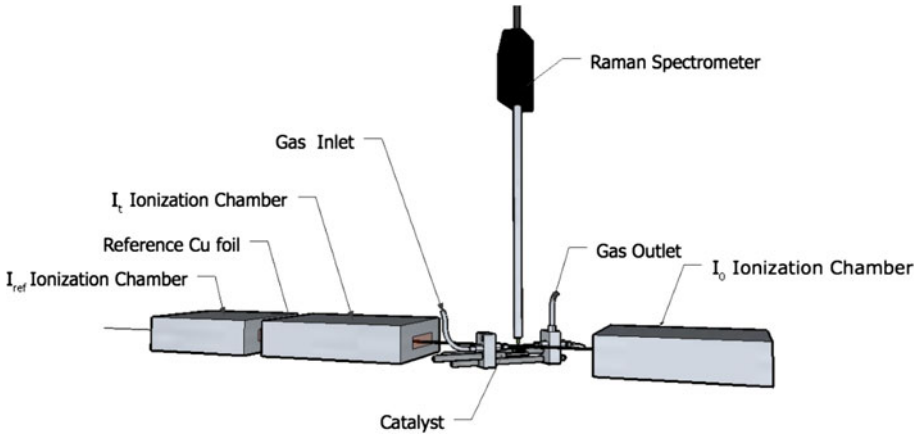

Fig. 1 Schematic of the setup for combined, *operando* XAS/Raman experiment

for measuring incident and transmitted beam intensities. In addition, a third ionization chamber was used to detect the beam through a reference Cu foil, for energy calibration and alignment purposes. Spectra obtained in the same conditions (from three to five spectra, depending on the temperature and conditions of the experiment) were averaged to minimize noise for further processing and analysis. XANES data were processed using linear combination analysis method, and EXAFS data were analyzed by non-linear least square fitting.

2.4 Raman Spectroscopy

Raman spectra were obtained by using a Bay Spec spectrometer equipped with a 532 nm laser excitation. The spectrometer was calibrated using a silicon wafer to a wavenumber accuracy of ± 1 cm^{-1}. Raman spectra were collected at the same temperatures as the XAS and MS data. A non-contact fiber optic HT probe objective was used for beam focusing and collection of scattered radiation (Fig. 1). 5 spectra were accumulated with a 30 s exposure time. The resulting total spectral recording time was 150 s. The laser output power was 23 mW. Raman spectra measured during a period of over 1 h, in which the catalyst was heated to the reaction temperature, did not show any observable changes, thus confirming the catalyst stability and the negligible effect of laser heating. Figure 1 demonstrates a schematic of the setup for combined, *operando* XAS/Raman investigations.

3 Results and Discussion

3.1 In Situ Reduction of Fresh 5 wt% CuO/TiO_2 Catalyst with CO

Figure 2a shows the Cu K-edge XANES data collected under a flow of CO. The data demonstrate that as the temperature increases, the oxidation state of Cu changes towards CuO, with the transformation almost complete by 100 °C. Figures 2b, c show the Cu K-edge k^2-weighted EXAFS data and their Fourier transform magnitudes, respectively. Figure 2c demonstrates a gradual decrease in the intensity of the lower *r* peak corresponding to the Cu–O bond between 1.1 and 2.0 Å from 25 to 50 °C. This decrease is followed by the rise of the higher *r* peak corresponding to the Cu–Cu first-nearest-neighbor distance in metallic Cu at higher temperatures. In perfect agreement with the XANES data, the transformation towards metallic Cu is almost complete by 100 °C.

Quantitative analysis of the EXAFS data measured at the highest temperature during reduction confirmed that the metal Cu phase dominates the data (Fig. 3). The data of bulk Cu foil was analyzed first, by a non-linear least square fit of FEFF6 theory [38] to the data by using Artemis program [39] from the IFEFFIT data analysis package [40]. Theoretical photoelectron scattering amplitudes and phase shifts were calculated for the fcc model structure corresponding to bulk Cu. Passive electron reduction factor was obtained to be 0.813 from the fit to bulk Cu foil data and, subsequently, fixed in the analysis of the unknown Cu data. The coordination numbers, correction to the bulk bond lengths, and the disorder in the bond lengths were varied in the fit to the first coordination shell EXAFS signal (Fig. 3), as well as the correction to the photoelectron energy origin. Best fit results confirmed our qualitative conclusion (vide supra) that a metal Cu phase was formed, with coordination numbers (CN) of Cu–Cu pairs of 12.0 ± 0.9. This large CN indicates that the particle size is at least 3–4 nm, consistent with TEM analysis results obtained on the as-received sample (with the average CuO_x particle size of about 3 nm).

Raman spectroscopy results are shown in Fig. 4. Raman spectra clearly demonstrate the presence of four bands around 147, 397, 517, and 638 cm^{-1} which correspond to anatase TiO_2 [30, 41–44]. No features around 232, 446, and

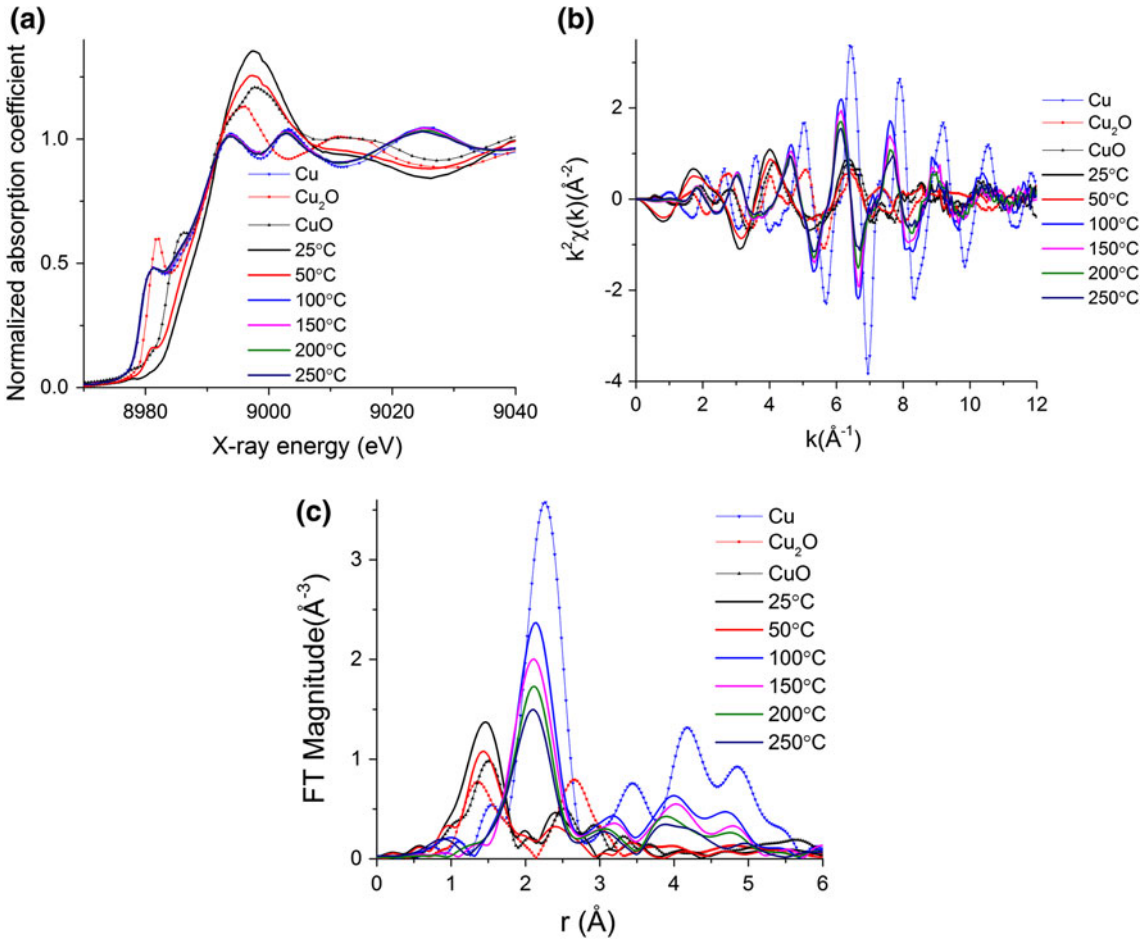

Fig. 2 Cu K-edge XANES (**a**) and EXAFS spectra in k-space (**b**) and r-space (**c**) collected for the CuO_x/TiO_2 catalyst at different temperatures under a flow of CO. The reference spectra of Cu, Cu_2O and CuO are shown as well

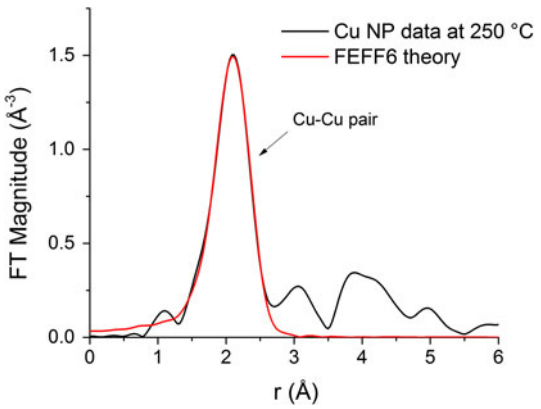

Fig. 3 Fourier transform magnitude of the k^2-weighted Cu K-edge EXAFS data and theoretical fit

609 cm^{-1} that correspond to the rutile TiO_2 phase [29] were observed. We cannot confirm or rule out the presence of CuO whose peak at 635 cm^{-1} [44–46] would interfere with the TiO_2 peak. The Cu_2O peak reported to be found at 411 cm^{-1} [46] is likely to be the peak at 418 cm^{-1} in Fig. 4. Additional evidence for this assignment is the absence of the 418 cm^{-1} peak in Raman spectra of pure TiO_2 (vide infra). Another peak of Cu_2O is expected to be found at 633 cm^{-1} [46], but its presence cannot be detected for the same reason as for the CuO peak, due to the interference with TiO_2.

It is remarkable that most spectral lines of TiO_2 have reduced significantly or even disappeared starting at 150 °C, the fact to be discussed in greater detail later. Another interesting observation is that the Cu_2O lines persist throughout the entire temperature cycle. This latter result is among the main advantages of using the XAS and Raman measurement in the same experiment. Indeed, Cu XANES and EXAFS data shown above are dominated by metal Cu and thus cannot be used for quantitative determination of CuO and/or Cu_2O phase that, if dilute, would have gone unnoticed by data analysis. However, metal Cu is not Raman active and, hence, the presence of Cu oxide will be detected even in minor quantities. By combining Raman and XAS we, therefore, conclude that both Cu and Cu_2O are present in the sample throughout the entire

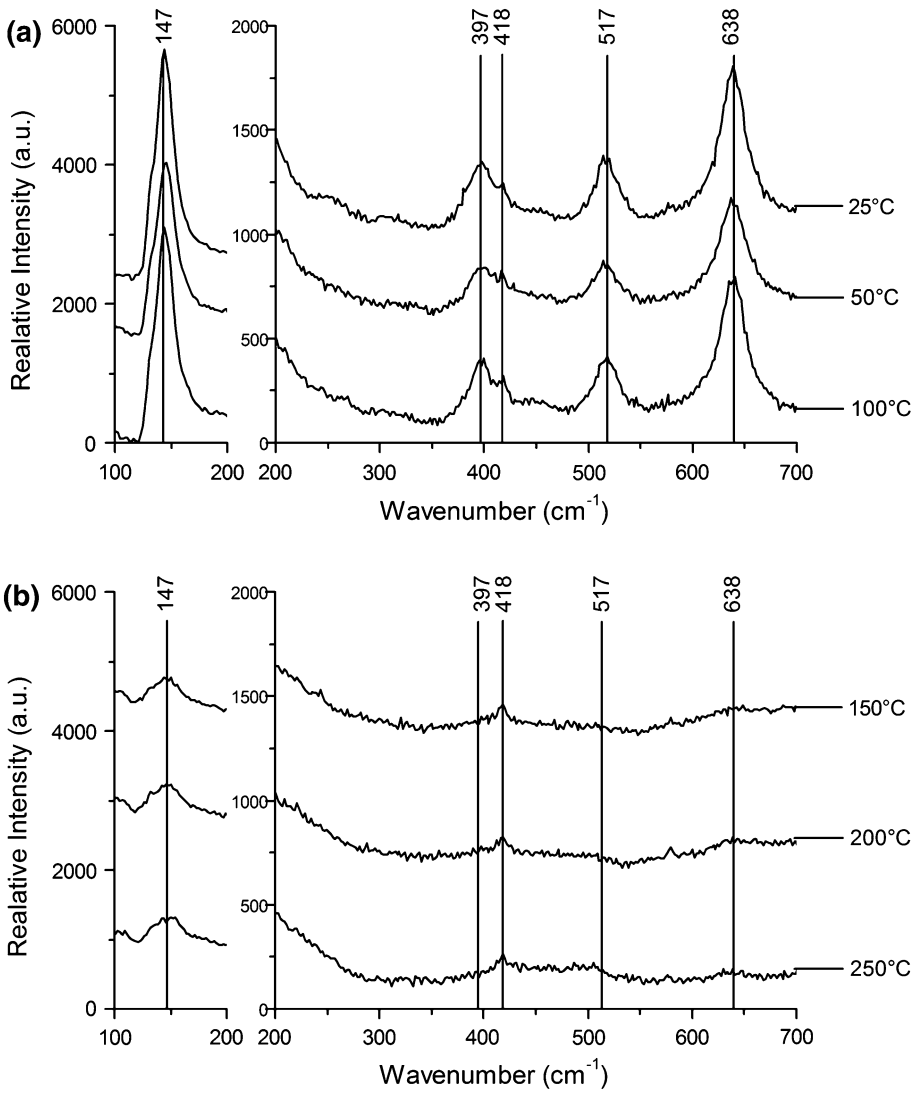

Fig. 4 Raman spectroscopy data collected during the reduction of the as-received catalyst with CO. All lines correspond to TiO_2 (anatase) except for the 418 cm^{-1} line which is due to Cu_2O. The data are divided in two groups, one–for temperatures from 25 to 100 °C (**a**), the other–for temperatures from 150 to 250 °C (**b**)

temperature range. This conclusion cannot be made on the basis of each individual technique, only on the basis of their combination, since XAS signals are dominated by metal Cu at the end of the reduction, while the Raman spectra do not have sensitivity to metal phase and, hence, enhance the oxide phase if it is present.

3.2 Oxidation of CO over a 5 wt% CuO/TiO_2 Catalyst as a Function of Temperature

We will start by showing the activity of CuO/TiO_2 for the oxidation of CO. Figure 5 displays different signals measured with the mass spectrometer after passing a mixture of $CO/O_2/He$ over the CuO/TiO_2 catalyst. A maximum in the production of CO_2, accompanied by the decrease in the CO and O_2 signals, is observed at a temperature of 150 °C. This result is in excellent agreement with those of Larsson et al. [44]. It took 3 h for the catalyst to reach 150 °C after the temperature was ramped up.

Figure 6a displays a series of Cu K-edge XANES spectra acquired after exposing a CuO_x/TiO_2 catalyst to the CO and O_2 mixture at different temperatures. It is apparent from visual examination of the spectra that the local environment and, likely, the oxidation state of Cu have changed during the reaction. For quantitative data analysis, we chose the same approach as in Ref. [19], where water–gas shift reaction over a Cu/CeO_2 inverse catalyst was investigated by XAFS *in operando*. As in the previous work, the starting state of Cu is not equivalent to that of CuO (or Cu_2O) as the former has strong spectroscopic differences in the 1s-4p transition region between 8,980 and 8,990 eV from the latter (Fig. 6a). Quantitative analysis of the mixing fraction of different species was obtained by linear combination fitting, similar to the procedure developed in Ref. [19]. In the present work, we used the starting phase as one of the standards, along with the spectra collected for bulk CuO and Cu_2O, to fit the unknown data at temperatures from 50 to 250 °C. The

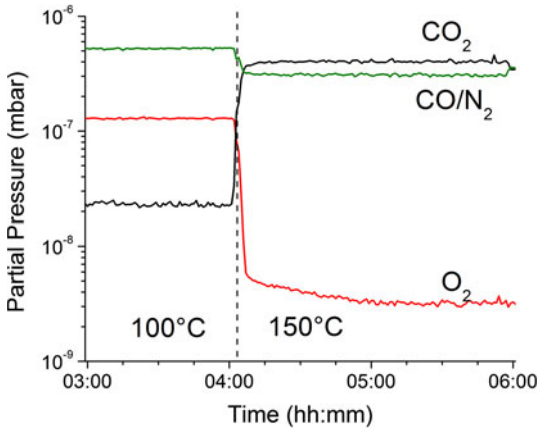

Fig. 5 Mass spectrometry data obtained for the CO oxidation reaction in the same experiment with XAS and Raman spectroscopy measurements

results of this analysis are presented in Fig. 6b. The changes in the XANES spectra are consistent with the transformation between the three states: (1) The starting state persisting between room temperature and 50 °C, (2) CuO-like state formed between 50 and 100 °C, and (3) Cu_2O-like state formed between 100 and 200 °C.

Theoretical fit to the 25 °C EXAFS spectra resulted in the coordination number of Cu–O of 3.7 ± 0.4 and the Cu–O pair distance of 1.95 ± 0.01 Å (Fig. 6b), i.e., consistent with bulk CuO structure. Despite that similarity, the difference in the XANES white line intensity and shape of the main edge between these two systems (Fig. 6a) is a clear evidence that the starting state is unique, and investigation of its nature should warrant a separate study. From the comparison of the reactivity data (Fig. 5) and XANES analysis data (Fig. 6b) we conclude that the starting phase

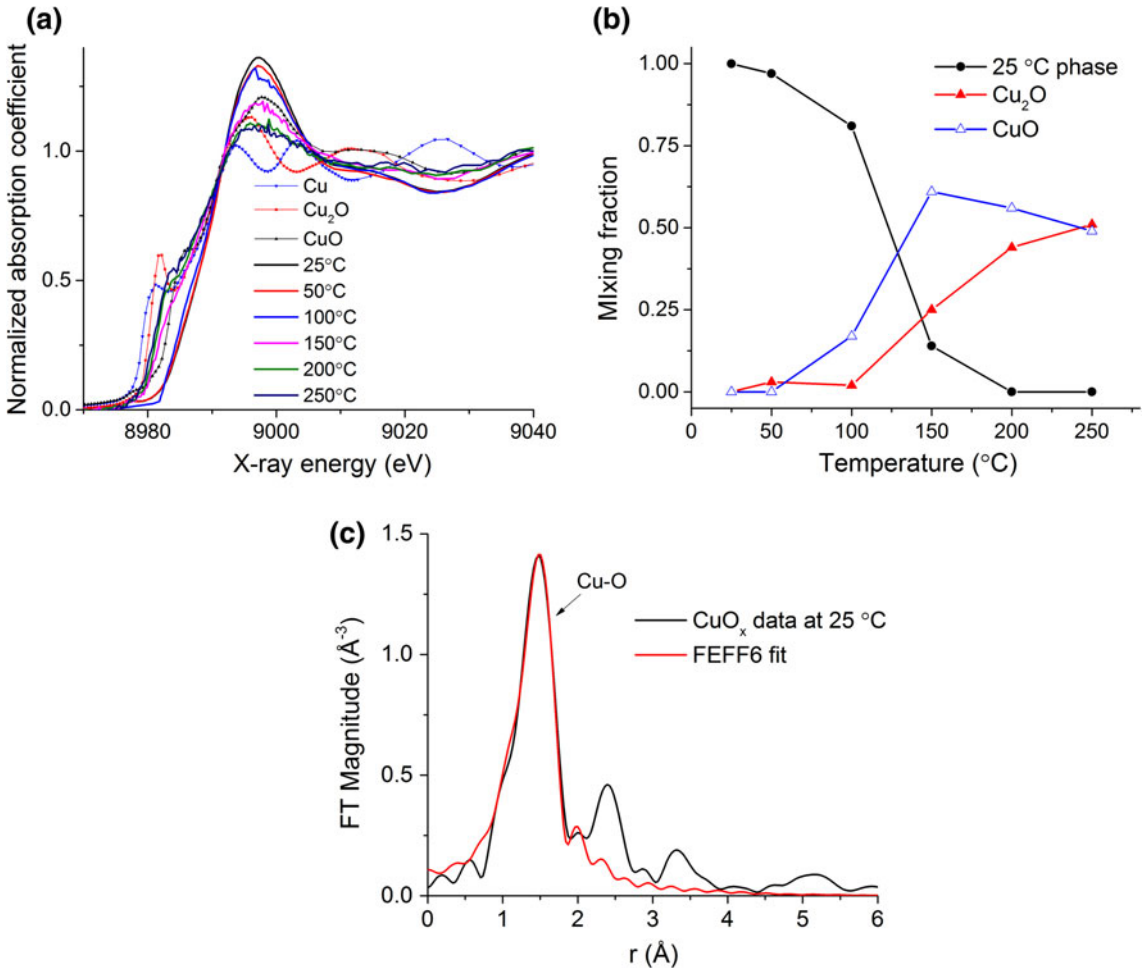

Fig. 6 Cu K-edge XANES spectra collected for a CuO_x/TiO_2 catalyst during the CO oxidation reaction (**a**). The corresponding reference spectra of Cu, Cu_2O and CuO are shown as well. The results of linear combination analysis of the XANES data with three standards: the pre-reaction phase at 25 °C, Cu_2O and CuO (**b**). Fourier transform magnitudes of k^2-weighted data and fit at 25 °C under O_2 flow, prior to the start of the CO oxidation reaction (**c**)

plays no role in reaction (as it almost disappears at 150 °C), and the reaction onset coincides with the formation of CuO and Cu_2O phases. We note that the XANES and EXAFS data were used in a complementary way in this work: while XANES is useful for phase speciation (by linear combination analysis), EXAFS data cannot be reliably analyzed when a mixture of species is present. However, such analysis is not necessary if each species can be analyzed separately, in their pure state, as in the present case [28, 47].

In summary of our analysis of the XAS and reactivity data (Fig. 5), we conclude that the active phase must consist of either CuO or Cu_2O or their mixture. Figure 7 shows the Raman spectra of the 5 wt% CuO/TiO_2 catalytic system measured during the course of the CO oxidation reaction, done in the same experiment with the other techniques described above.

Raman spectra show that Cu_2O state is present in the sample at all temperatures, while CuO cannot be reliably detected due to the interference with TiO_2. On the basis of Raman spectra alone we would not be able to detect the unique state of Cu in the beginning of the temperature range, visible in XAS spectra (Fig. 6a,b). Hence, the combination of XAS and Raman spectra is required for more accurate speciation of multiple Cu species that coexist in the catalyst during this reaction.

Figure 8a shows the Raman spectra collected in the same TiO_2 powder that was used as a support for the 5 wt% CuO/TiO_2 catalyst, but no CuO was present in that sample. Correspondingly, no conversion of CO to CO_2 was observed (Fig. 8b). The Raman spectra of the pure TiO_2 sample (Fig. 8a) also indicates the anatase phase, in agreement with Fig. 7. It is important that the spectra show no presence of the peak at 418 cm^{-1}, in support of its assignment to Cu_2O as discussed above. Interestingly, the peak intensities measured in the pure TiO_2 sample do not change significantly with temperature (Fig. 8 (a)), in a marked contrast with their behavior measured in the 5 wt% CuO/TiO_2 catalyst during its reduction with CO. In the latter sample, the TiO_2 peak intensities decrease

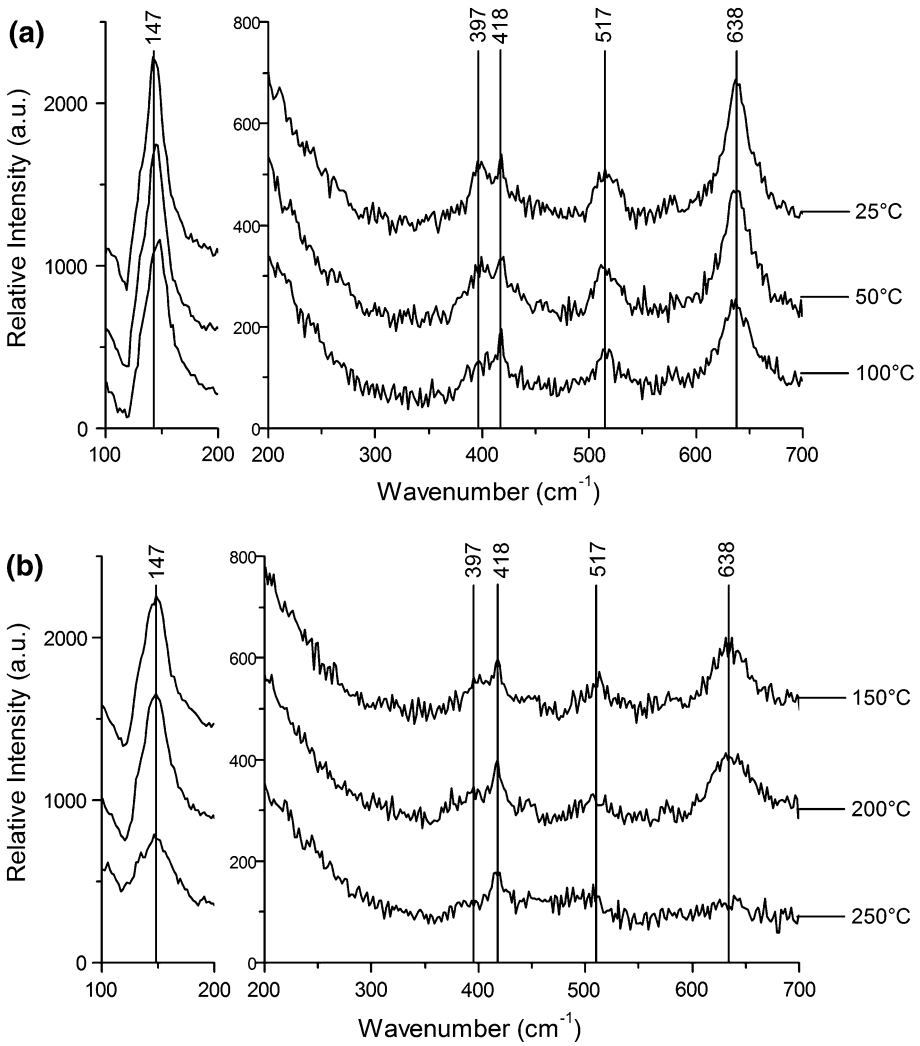

Fig. 7 Raman spectra obtained during the CO oxidation reaction cycle. All lines correspond to TiO_2 (anatase) except for the 418 cm^{-1} line which is due to Cu_2O. The data are divided in two groups, one–for temperatures from 25 to 100 °C (**a**), the other–for temperatures from 150 to 250 °C (**b**)

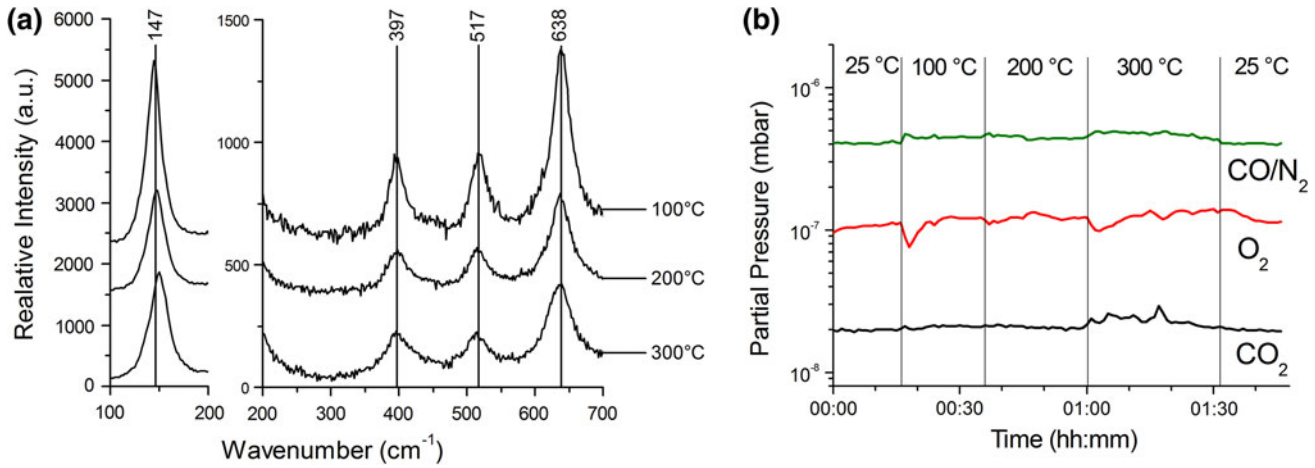

Fig. 8 Raman spectra of pure TiO_2 catalyst collected during the reaction cycle (**a**). Mass spectrometry data demonstrating the lack of CO conversion when pure TiO_2 was used (**b**)

dramatically (Fig. 4). This contrast in Raman spectra behavior illuminates a special role that the substrate (TiO_2) plays in the reduction of copper oxide.

The final experiment that we performed, where the reactant mixture for the water–gas shift (CO and H_2O) was flown over a fresh catalyst in the same temperature and flow rate regimes as in the previous two experiments, demonstrated CO oxidation and the lack of evolution of H_2. Hence, this catalyst shows no activity for the water–gas shift reaction.

4 Summary

The combined application of spectroscopic techniques (XANES, EXAFS and Raman) done *in operando*, during a catalytic process of CO oxidation, revealed new information about the nature of the catalytically active phase and its heterogeneity. Results of all complementary measurements suggest that both phases of copper oxide (CuO and Cu_2O) must be present in the active state of the catalyst at 200 °C.

Raman studies highlighted the role that the support material (TiO_2) plays in this reaction. Under the conditions when oxygen is deficient, TiO_2 played a role as an oxygen reservoir, providing oxygen for the oxidation of CO. Our studies reveal also the synergy between the Cu oxide and the support, since TiO_2 acts as oxygen source only in the presence of the Cu oxide. Our results illustrate that novel chemical and catalytic properties can appear when two different oxides are put in contact at the microscopic level.

Acknowledgments The authors are grateful to L. Barrio for preparing the catalyst used in this work. AIF and AP acknowledge the support of this work by the U.S. DOE Grant No. DE-FG02-03ER15476. X19A beamline is supported, in part, by Synchrotron Catalysis Consortium (U.S. DOE Grant No. DE-FG02-05ER15688). The work carried out at the Chemistry Department of BNL was supported by the U.S. Department of Energy, Chemical Science Division (DE-AC02-98CH10886).

References

1. Leyva C, Rana MS, Ancheyta J (2008) Catal Today 130:345
2. Montanari T, Marie O, Daturi M, Busca G (2005) Catal Today 110:339
3. Stuchinskaya TL, Kozhevnikov IV (2003) Catal Commun 4:609
4. Noronha FB, Schmal M, Primet M, Frety R (1991) Appl Catal 78:125
5. Karpiński Z (1990) In: Eley DD, Pines H, Weisz PB (eds) Advances in catalysis, vol 37. Academic Press, London, p 45
6. Valden M, Lai X, Goodman DW (1998) Science 281:1647
7. Liu W, Wadia C, Flytzani-Stephanopoulos M (1996) Catal Today 28:391
8. Edwards MA, Whittle DM, Rhodes C, Ward AM, Rohan D, Shannon MD, Hutchings GJ, Kiely CJ (2002) Phys Chem Chem Phys 4:3902
9. Rao GR, Kašpar J, Meriani S, Monte R, Graziani M (1994) Catal Lett 24:107
10. Sinfelt JH, Meitzner GD (1993) Acc Chem Res 26:1
11. Anderson MW, Klinowski J (1990) J Am Chem Soc 112:10
12. Sojka Z, Che M (2001) Appl Magn Reson 20:433
13. Leba A, Davran-Candan T, Önsan ZI, Yıldırım R (2012) Catal Commun 29:6
14. Ren B, Lin X-F, Yang Z-L, Liu G-K, Aroca RF, Mao B-W, Tian Z-Q (2003) J Am Chem Soc 125:9598
15. Lietz G, Lieske H, Spindler H, Hanke W, Völter J (1983) J Catal 81:17
16. Grunwaldt J-D, Clausen BS (2002) Top Catal 18:37
17. Frenkel AI, Rodriguez JA, Chen JG (2012) ACS Catal 2:2269
18. Shannon IJ, Maschmeyer T, Sankar G, Thomas JM, Oldroyd RD, Sheehy M, Madill D, Waller AM, Townsend RP (1997) Catal Lett 44:23
19. Frenkel AI, Wang Q, Marinkovic N, Chen JG, Barrio L, Si R, López Cámara A, Estrella AM, Rodriguez JA, Hanson JC (2011) J Phys Chem C 115:17884
20. Weckhuysen BM (2003) Phys Chem Chem Phys 5:4351

21. Tinnemans SJ, Mesu JG, Kervinen K, Visser T, Nijhuis TA, Beale AM, Keller DE, van der Eerden AMJ, Weckhuysen BM (2006) Catal Today 113:3
22. Beale AM, van der Eerden AMJ, Jacques SDM, Leynaud O, O'Brien MG, Meneau F, Nikitenko S, Bras W, Weckhuysen BM (2006) J Am Chem Soc 128:12386
23. Mesu JG, van der Eerden AMJ, de Groot FMF, Weckhuysen BM (2005) J Phys Chem B 109:4042
24. Tromp M, Sietsma JRA, van Bokhoven JA, van Strijdonck GPF, van Haaren RJ, van der Eerden AMJ, van Leeuwen PWNM, Koningsberger DC (2003) Chem Commun, 128
25. Newton MA, Dent AJ, Fiddy SG, Jyoti B, Evans J (2007) Catal Today 126:64
26. Newton MA, van Beek W (2010) Chem Soc Rev 39:4845
27. Marinkovic NS, Wang Q, Frenkel AI (2011) J Synchrotron Radiat 18:447
28. Patlolla A, Carino EV, Ehrlich SV, Stavitski E, Frenkel AI (2012) ACS Catal 2:2216
29. Wainwright MS, Foster NR (1979) Catal Rev 19:211
30. Busca G, Ramis G, Amores JMG, Escribano VS, Piaggio P (1994) J Chem Soc Faraday Trans 90:3181
31. Breen JP, Ross JRH (1999) Catal Today 51:521
32. Takezawa N, Iwasa N (1997) Catal Today 36:45
33. Larsson P-O, Andersson A (2000) Appl Catal B 24:175
34. Dong G, Wang J, Gao Y, Chen S (1999) Catal Lett 58:37
35. Kumar PM, Badrinarayanan S, Sastry M (2000) Thin Solid Films 358:122
36. Schalow T, Brandt B, Laurin M, Guimond S, Starr D, Shaikhutdinov S, Schauermann S, Libuda J, Freund H-J (2007) Top Catal 42–43:387
37. Clausen BS, Steffensen G, Fabius B, Villadsen J, Feidenhans'l R, Topsøe H (1991) J Catal 132:524
38. Zabinsky SI, Rehr JJ, Ankundinov A, Albers RC, Eller MJ (1995) Phys Rev B 52:2995
39. Ravel B, Newville M (2005) J Synchrotron Radiat 12:537
40. Newville MJ (2001) Synchrotron Radiat 8:322
41. Larsson P-O, Andersson A (1998) J Catal 179:72
42. Kosuge K (1999) J Phys Chem B 103:3563
43. Schramlmarth M, Wokaun A, Baiker A (1991) Fresen J Anal Chem 341:87
44. Larsson P-O, Andersson A, Wallenberg LR, Svensson B (1996) J Catal 163:279
45. Reimann K, Syassen K (1990) Solid State Commun 76:137
46. Hamilton JC, Farmer JC, Anderson RJ (1986) J Electrochem Soc 133:739
47. Wang Q, Hanson JC, Frenkel AI (2008) J Chem Phys 129:234502